

Electronic Supplementary Information for: Cyclo[18]carbon including Zero-Point Motion: Ground State, First Singlet and Triplet Excitations, and Hole Transfer

Konstantinos Lambropoulos^{*,a}, Antonios M. Alvertis^{b,c}, Andreas Morphis^a, and Constantinos Simserides^a

^aDepartment of Physics, National and Kapodistrian University of Athens, Panepistimiopolis, Zografos GR-15784, Athens, Greece. Email: klambro@phys.uoa.gr, amorphis@phys.uoa.gr, csimseri@phys.uoa.gr

^bCavendish Laboratory, University of Cambridge, J. J. Thomson Avenue, Cambridge CB3 0HE, United Kingdom. Email: ama80@cam.ac.uk

^cMaterials Sciences Division, Lawrence Berkeley National Laboratory, Berkeley, California 94720, USA.

Additional Figures

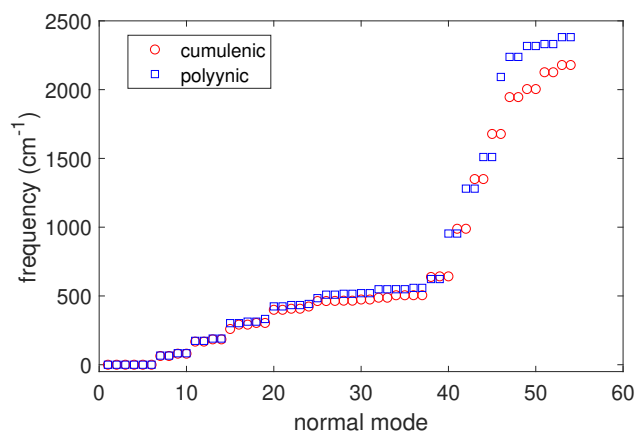


Figure S1: Vibrational analysis of cumulenic (empty red circles) and polyynic (empty blue squares) cyclo[18]carbon, with the cc-pVTZ basis set.

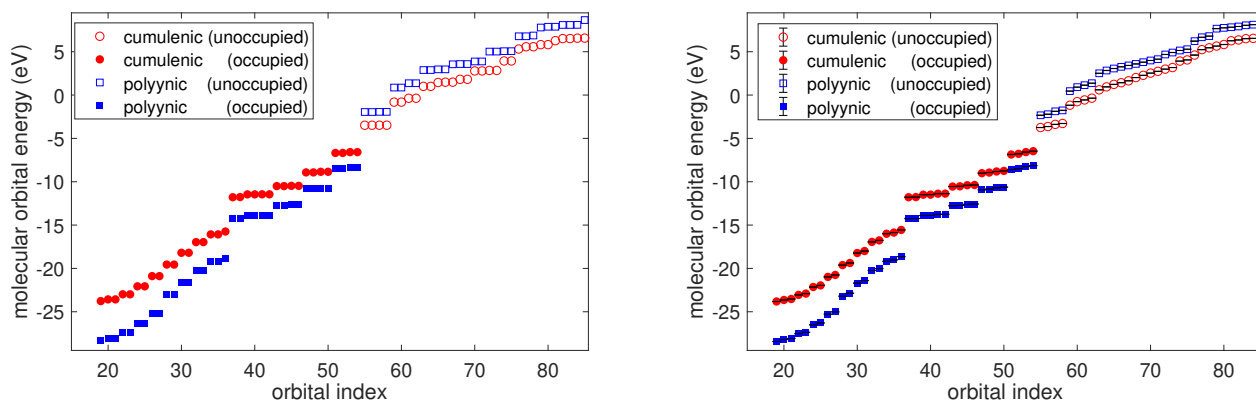


Figure S2: Energies of several occupied (filled shapes) and unoccupied (empty shapes) orbitals of cumulenic (red circles) and polyynic (blue squares) cyclo[18]carbon. (Left) Static conformations. (Right) Averaged values of the Monte Carlo sample, accounting for zero-point vibrations, including standard errors.

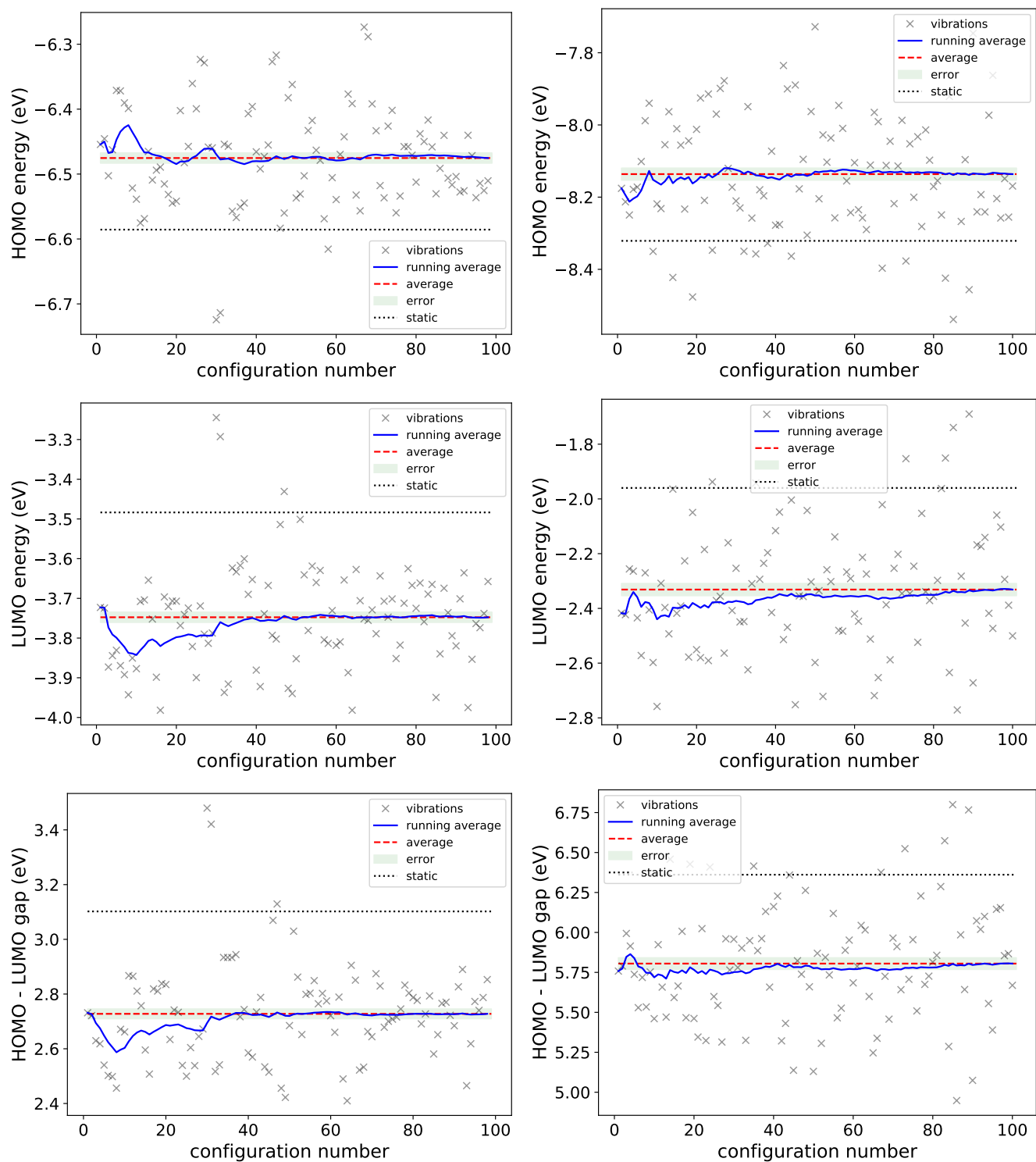


Figure S3: Comparison of the HOMO energy (first row), LUMO energy (second row), and HOMO-LUMO gap (third row) of static cumulenyl (left column) and polynic (right column) cyclo[18]carbon with their corresponding renormalized values due to zero-point vibrations, using the Monte Carlo method. The values for each Monte Carlo configuration and the running averages are also shown.

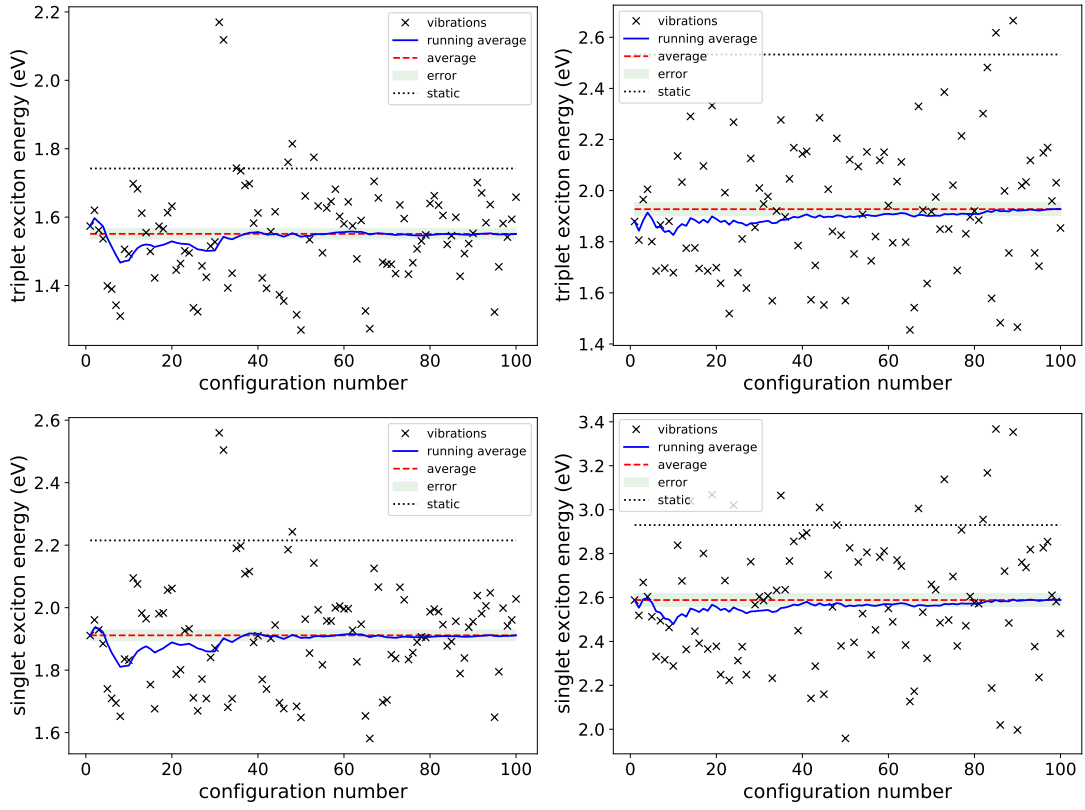


Figure S4: Comparison of the first triplet (first row) and first singlet (second row) excitation energies of static cumulenic (left column) and polynic (right column) cyclo[18]carbon with their corresponding renormalized values due to zero-point vibrations, using the Monte Carlo method. The values for each Monte Carlo sample and the running averages are also shown.

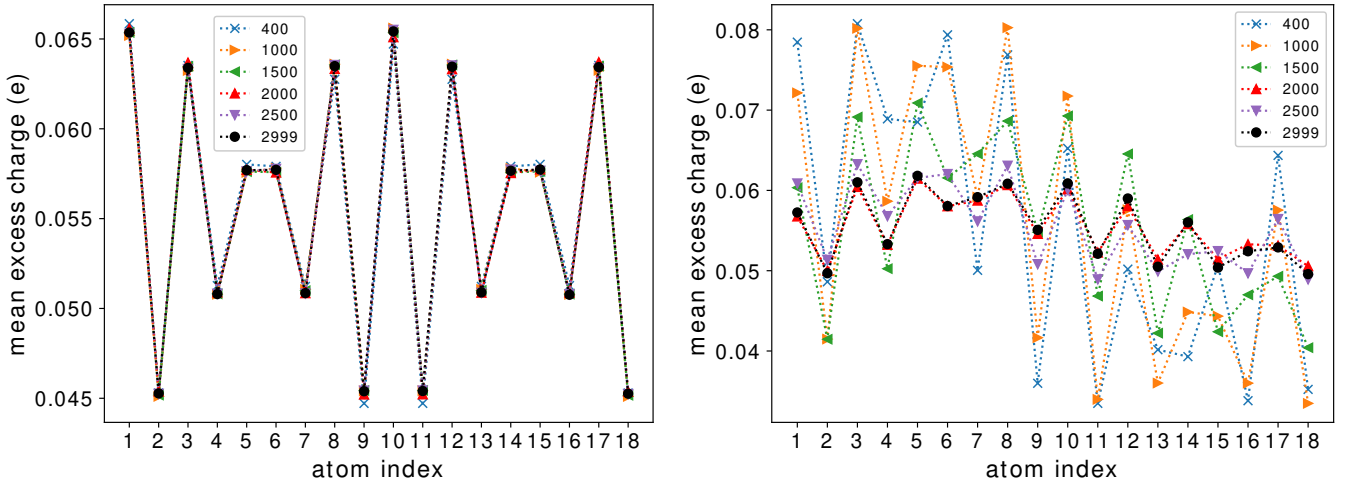


Figure S5: Time-convergence of the mean excess charge distribution of static cumulenic (left) and polynic (right) cyclo[18]carbon. Time intervals are specified in the legend, in atomic units. Dotted lines are guide for the eye.

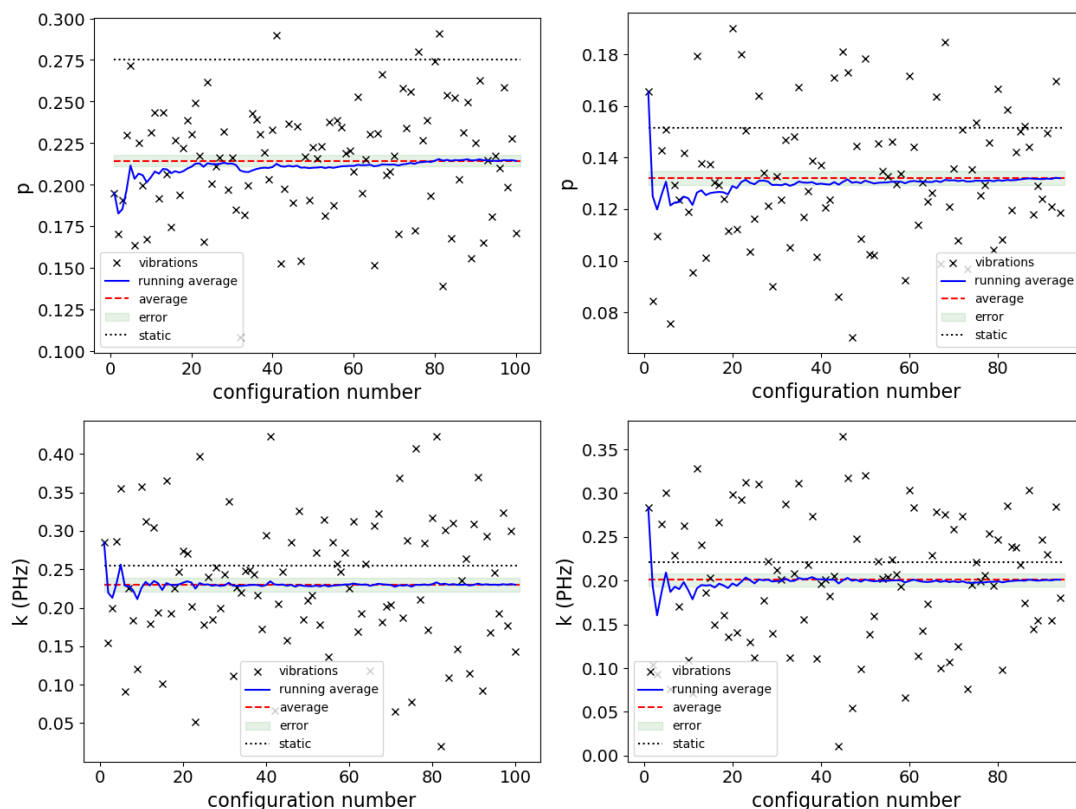


Figure S6: Comparison of the maximum value of excess charge, p , at the diametrically opposed atom to the one the hole was initially placed (first row) and the mean transfer rate, k , (second row) of static cumulenenic (left column) and polyyenic (right column) cyclo[18]carbon with their corresponding renormalized values due to zero-point vibrations, using the Monte Carlo method. The values for each sample and the running averages are also shown.

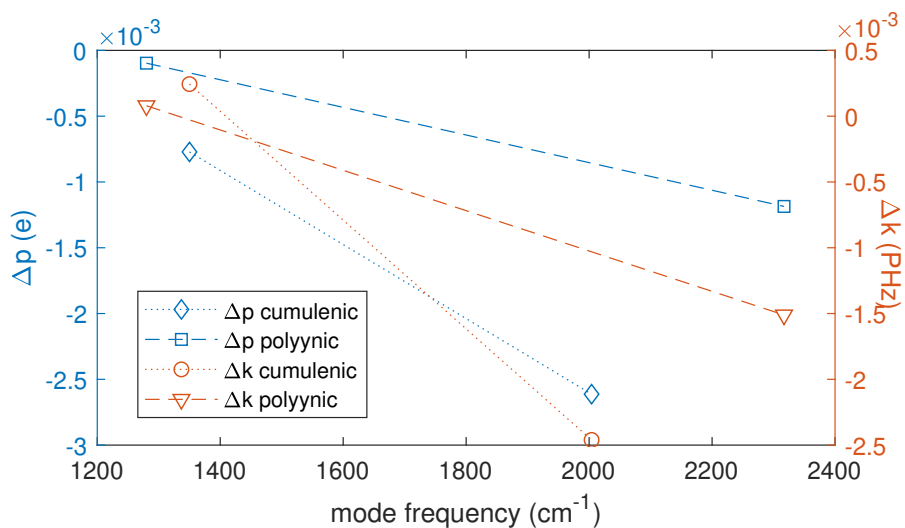


Figure S7: Contribution of the modes at $\approx 2004 \text{ cm}^{-1}$ ($\approx 2317 \text{ cm}^{-1}$) and $\approx 1350 \text{ cm}^{-1}$ ($\approx 1280 \text{ cm}^{-1}$) which display major and minor contributions, respectively, on the HOMO-LUMO gaps, and T_1 and S_1 excitation energies [cf, Fig. 2(d)-(e) of the main text], for cumulenenic (polyyenic) cyclo[18]carbon, within the quadratic method.